NIH Public Access
Author Manuscript
J Bone Miner Res. Author manuscript; available in PMC 2014 September 05.

Published in final edited form as:
J Bone Miner Res. 2012 March ; 27(3): 702–712. doi:10.1002/jbmr.1497.

Parathyroid hormone treatment improves the cortical bone micro-structure by improving the distribution of type I collagen in postmenopausal women with osteoporosis

Maria-Grazia Ascenzi[1], **Vivian P. Liao**[1], **Brittany M. Lee**[1], **Fabrizio Billi**[1], **Hua Zhou**[2], **Robert Lindsay**[2,3], **Felicia Cosman**[2,3], **Jeri Nieves**[2,4], **John P. Bilezikian**[3], and **David W. Dempster**[2,5]

Maria-Grazia Ascenzi: mgascenzi@mednet.ucla.edu; Vivian P. Liao: vivian.p.liao@gmail.com; Brittany M. Lee: brittanylee2011@gmail.com; Fabrizio Billi: fbilli@laoh.ucla.edu; Hua Zhou: zhouh@helenhayeshosp.org; Robert Lindsay: lindsayr@helenhayeshosp.org; Felicia Cosman: cosmanf@helenhayeshosp.org; Jeri Nieves: nievesj@helenhayeshosp.org; John P. Bilezikian: JPB2@columbia.edu; David W. Dempster: dempster@helenhayeshospital.org

[1]UCLA/Orthopaedic Hospital Department of Orthopaedic Surgery, University of California at Los Angeles

[2]Regional Bone and Clinical Research Centers, Helen Hayes Hospital, West Haverstraw, NY

[3]Department of Medicine, School of Public Health, College of Physicians and Surgeons, Columbia University, New York

[4]Department of Division of Epidemiology, School of Public Health, College of Physicians and Surgeons, Columbia University, New York

[5]Department of Pathology, School of Public Health, College of Physicians and Surgeons, Columbia University, New York

Abstract

Although an important index, the level of bone mineral density (BMD) does not completely describe fracture risk. Another bone structural parameter, the orientation of type I collagen, is known to add to risk determination, independently of BMD, ex vivo. We investigated the Haversian system of transiliac crest biopsies from postmenopausal women before and after treatment with parathyroid hormone (PTH). We used the birefringence of circularly polarized light and its underlying collagen arrangements by confocal and electron microscopy, in conjunction with the degree of calcification by high-resolution micro-X-ray. We found that PTH treatment increased the Haversian system area by 48.28±38.78%; decreased bright birefringence from 0.45±0.02 to 0.40±0.01 (scale zero to one, p=0.0005); increased the average percent area of osteons with alternating birefringence from 48.15±10.27 to 66.33±7.73 (p=0.034), decreased non-

Corresponding author: Maria-Grazia Ascenzi, Department of Orthopedic Surgery, University of California at Los Angeles, Rehabilitation Bldg, Room 22-69, 1000 Veteran Avenue, Los Angeles, CA 90095, Tel. 310/825-6341, Fax 310/825-5290, mgascenzi@mednet.ucla.edu.

Dr. Ascenzi is the inventor under granted and pending published patent applications related to her bone micro-structural research, the rights to which are licensed to Micro-Generated Algorithms, LLC, a California limited liability company in which she holds an interest. Dr. Lindsay declares the following financial relationships: Amgen, Lilly Novartis. Dr. Cosman has obtained research support from Eli Lilly and Novartis, and is a consultant, advisor and/or speaker for Eli Lilly, Merck, Novartis, Amgen and Zosano. Dr. Bilezikian is a consultant for Eli Lilly, Novartis, Amgen, Warner Chilcott, NPS Pharmaceuticals, Merck and Radius Pharmaceuticals. Dr. Dempster has obtained research support from Eli Lilly, and is a consultant and/or speaker for Eli Lilly, Merck & Co, Amgen Inc, and NPS Pharmaceuticals. All other authors have no conflicts of interest.

NIH-PA Author Manuscript
NIH-PA Author Manuscript
NIH-PA Author Manuscript

NIH-PA Author Manuscript

NIH-PA Author Manuscript

NIH-PA Author Manuscript

significantly the semi-homogeneous birefringent osteons (8.36±10.63 vs. 5.41±9.13, p=0.40) and birefringent bright (4.14±8.90 vs. 2.08±3.36, p=0.10) osteons. Further, lamellar thickness significantly increased from 3.78±0.11μm to 4.47±0.14μm (p=0.0002) for bright, and from 3.32±0.12μm to 3.70±0.12μm (p=0.045) for extinct, lamellae. This increased lamellar thickness altered the distribution of birefringence and therefore the distribution of collagen orientation in the tissue. With PTH treatment, a higher percent area of osteons at initial degree of calcification was observed, relative to intermediate-low degree of calcification (57.16±3.08 vs. 32.90±3.69, p=0.04), the percentage of alternating osteons at initial stages of calcification increasing from 19.75±1.22 to 80.13±6.47, p=0.001. In conclusion, PTH treatment increases heterogeneity of collagen orientation, a starting point to study the reduction in fracture risk when PTH is used to treat osteoporosis.

Keywords

bone histomorphometry; collagen; osteoporosis; novel entities <treatment>

Introduction

The anabolic effect of human PTH(1-34) in osteoporosis has been a major focus of interest since the 1970s.[1–8] Intermittent use of PTH(1-34) (once daily for 18–24 months) decreases vertebral and non-vertebral fracture risk in patients[5,9,10] and improves bone microstructure and strength in animal models.[11–15] Further, PTH(1–34) administration has been found in animal models to facilitate bone repair after fracture[16–20] and spinal fusion.[21]

The anabolic action of PTH on bone has been found to vary with respect to compact and cancellous compartments. Cancellous bone volume in iliac crest biopsies from subjects treated with PTH(1-34) does not consistently increase,[22,23] while cortical volume, thickness and endocortical wall width do increase significantly in postmenopausal women on PTH(1-34).[23–25] Recent experiments suggest that PTH increases the number of mesenchymal stem cells and stimulates vascular endothelial growth factor.[26,27] In addition, PTH has been found to act as a pro-differentiation and anti-apoptopic agent on osteoblasts by reducing osteocytic sclerostin and Dkk1.[28–30] Such inhibition would lead to a stimulation of Wnt and Bmp anabolic pathways, accounting for some of the skeletal changes.[31–34]

Since cortical bone forms 80% of the adult skeleton,[35] is a major contributor to bone strength,[36,37] and is increased by PTH treatment, we asked whether the compact micro-structure is similar or different in the comparison of before and after treatment. This investigation was guided by two observations. First, the increased thickness of cortical bone following PTH(1-34) treatment indicated that the osteons formed during treatment may increase the percentage of osteons at initial stages of calcification. We use the term “calcification” throughout this paper “with reference to a process which leads to the formation of a solid, stable, amorphous or crystalline inorganic phase in the context of intra- and/or extra-cellular organic structure”.[38] This first observation led us to investigate the degree of calcification of the osteon. Second, we drew upon a set of three biomechanical

NIH-PA Author Manuscript

NIH-PA Author Manuscript

NIH-PA Author Manuscript

findings: 1] PTH(1-34) treatment was found to be associated with a reduced incidence of fractures in osteoporotic patients, and improved bone micro-structure and strength in animal models;[5–11] 2] patients with femoral neck fracture showed, at the fracture site, an altered lamellar thickness,[39] which is indicative of altered distribution of collagen type I orientation;[40–41] 3] fracture is delayed in human cortical microstructure ex vivo by a 1.5 to 2-fold amplification of elastic range and a 3-fold increase in stiffness by orientation of collagen type I.[42] This set of findings allows us to hypothesize that after treatment the bone tissue shows an altered distribution of collagen orientation and of degree of calcification. Since the molecular pathway by which Wnt and Bmp under PTH treatment affect the cortical micro-structural parameters mentioned here is unknown, the biomechanical motivation that underlies our hypothesis serves to identify a phenomenon that merits investigation from a molecular biology perspective.

The orientation of collagen and locally parallel carbonated hydroxyapatite within the lamellae are fundamental to rendering the mechanical properties of single osteons suitable to specific types of loading.[42] The study of cortical micro-structure can be dated back to Galileo, who first hypothesized the importance of bone micro-structure in determining macro-structural strength,[43] by virtue of provision of reinforcement in the preferential direction of the vascular canals. The study of osteons' lamellar components has involved numerous investigators since the first observation of lamellae by Leeuwenhoek in the late 1600's.[44] In health and in the presence of specific bone pathologies, collagen-apatite architecture has been found to adapt to local mechanical requirements and to show a heterogeneous non-random pattern throughout the macro-structure.[45] From a material science perspective, a material that shows reinforcements that vary in orientation and density in response to the local mechanical environment, with changeable orientation and intensity, delays occurrence of fracture more successfully than an isotropic homogenous material.

Material and Methods

This study uses bone biopsy material collected as part of an ongoing clinical trial designed to evaluate the effects of PTH(1-34) on bone structure and dynamic behavior, as well as the interaction of PTH(1-34) with antiresorptive agents such as bisphosphonates.[25] In 8 postmenopausal women with osteoporosis, transiliac crest bone biopsies were obtained before and after treatment with daily injections of 400 U of PTH(1-34) for 36 months. All subjects were on a chronic, stable dose of estrogen therapy throughout the duration of the study. Table 1 summarizes the age and previously reported cortical variables from the iliac crest bone biopsies obtained in that study and used in this investigation. Bone biopsies were embedded, cut, and prepared according to previously published methods.[46]

The Haversian system of each of the two cortices per section, one section per biopsy, was investigated. We considered the osteons as secondary osteons because the usually smaller primary osteons were not found here.[47] We investigated, in this order, the degree of calcification by micro-X-ray and the birefringent signal of circularly polarized light (CPL), whose underlying collagen orientation was observed at higher resolution by scanning confocal microscopy (SCM), and scanning transmission electron microscopy (STEM). The

NIH-PA Author Manuscript

NIH-PA Author Manuscript

NIH-PA Author Manuscript

observers were blind to whether each specimen was obtained before or after PTH(1-34) treatment.

High-resolution micro-X-radiography

This method was used to observe osteons formed during PTH(1-34) treatment and at various degrees of calcification at the maximum resolution available. We prepared the high-resolution (from 1 to 1.5μm) micro-X-ray with a micro-focus microradiograph (Ital-Structures, Riva del Garda-Trento, Italy) and high resolution glass plates (Microchrome Technology, San Jose, California) according to published methods.[47–50] In particular, an aluminum scale was micro-X-rayed with the bone section to provide a calibration for quantification of calcification.

Regular light and CPL microscopies

Each micro-X-ray (Fig. 1) and corresponding section, after rehydration with distilled water on non-cover slipped slide, were observed with a Leitz Dialux 20 (Midland, Ontario, Canada) from 100 to 160x. We labeled an osteon “whole” if it included a Haversian canal, whether complete or not. We took partially overlapping images of the entire cortices by regular light (RL) and CPL at maximum light intensity and by RL on micro-X-rays at 160x. We imported the images in XaraX software (Xara Group Ltd, London, England) stacked in three virtual layers (RL, CPL of section and RL of micro-X-ray) and reconstructed the three layers of each cortex. On a separate virtual layer, we traced the outer boundary of the cortex and of each osteon at the cement line. On a second, separate virtual layer of the stack, to assess lamellar thickness we drew segments in triplicate at 500x, across each bright and extinct lamella of alternating osteons. We exported each of the three reconstructed images and each of the layers with tracing from XaraX at 300 dpi for good resolution.

We calibrated MetaMorph software (Molecular Devices, Sunnyvale, California, United States) to measure in real microns. We programmed Metamorph to 1] open five images per cortex (RL and CPL of section, RL of micro-X-ray, two images with osteon tracing and lamellar thickness tracing) and arrange them in a virtual stack; 2] measure the area of the cortex and of each osteon; 3] assess the percentage of osteons and of interstitial bone at specific stages of calcification on a scale from 0 to 1: initial stage (0 to 0.24), intermediate-low stage (0.25 to 0.49), intermediate-high stage (0.5 to 0.74) and final stage (0.75 to 1); 4] measure the cortical porosity as the total area of Haversian canals plus resorption spaces, expressed as a percentage of the total area of the cortex; and 5] calculate the average birefringent brightness of the Haversian system on each cortex with a built-in function, as the sum of the grey values divided by the number of pixels after calibrating on a scale from 0 to 1, with 0 being completely extinct and 1 brightest.

To confirm visual assessment and to assess heterogeneity of birefringence of individual whole ostens, we thresholded the CPL image within the top half of the grey scale from 0 to 1 to mean “bright”. Metamorph colored in orange the bright regions, allowing us to classify and count osteons as “alternate” (alternating bright and extinct lamellae), “semi-homogeneous“ (containing bright or extinct regions that span portions of lamellae) and “bright” (completely bright). Because so-called “extinct” osteons always show a small 3 to

NIH-PA Author Manuscript

NIH-PA Author Manuscript

NIH-PA Author Manuscript

4% of bright lamellae around the Haversian canal,[42] they were denominated here as “semi-homogeneous”. We programmed Maple software to 1] measure the segments, previously drawn with XaraX software, representing lamellar thickness of alternate osteons and to assess the percentages of alternate osteons at specific stages of calcification by sorting alternate osteons by degree of calcification; and 2] sort the osteons by CPL appearance (alternate, semi-homogeneous, bright) and by degree of calcification (initial, intermediate-low, intermediate-high, final) and compute percentage for each combination of CPL appearance and degree of calcification.

Because in extinct field, the bright and extinct signals of birefringence are indicative of difference in organization of type I collagen,[40,41] the collagen orientation ranges underlying each of the bright and extinct birefringent signals were investigated by SCM and STEM.

Scanning confocal microscopy (SCM)

After rehydration with distilled water, each section was observed by a TCS-SP microscope (Leica Microsystems GmbH) with a krypton laser (568 nm excitation), 20x and 63x Planapochromat lens, and 580 to 700 nm detection wavelength range. The endogenous fluorescence of collagen provided good contrast on an extinct background of glycosaminoglycans and glycoproteins.[41,51] Light detected by photomultipliers was converted to pseudo-color for good visualization. Each section was scanned every 0.5μm to avoid either overlap or gaps between subsequent images. Stacks of images were collected automatically. We chose the same regions through the scanned image stack, covering 100μm x 100μm of the specimen in correspondence to regions of either brightness or extinction birefringence by CPL.

Collagen bundles appeared on the plane of focus as dots or segments, indicative of a range of orientations with respect to the direction perpendicular to the plane of the section.[41] A dot indicated collagen oriented longitudinally with respect to the transverse section observed by SCM, that is parallel to the Haversian canal direction. A segment was indicative of collagen not perpendicular to the transverse section. We distinguished dots from segments by identifying the dots as elements with width to length ratio up to 1.2; and the segments as elements with width to length ratio greater than 1.2. We marked the collagen bundles as dots and segments with XaraX software. We programmed Metamorph software to 1] measure with built-in functions width and length of the labeled elements in real microns; and 2] compute the percentage of dots and the percentage and length of segments. We conducted this analysis for bright and extinct regions separately.

Scanning transmission electron microscopy (STEM)

We prepared the bone specimens for transmission electron microscopy (TEM) following standard methods.[52] The sections were dehydrated and embedded in Araldite® (Huntsman Advanced Materials Americas Inc., Los Angeles, California). Ultra-thin 70-80nm serial sections parallel to the Haversian canal direction were prepared with an MT-1 Ultra Microtome (DuPont Instruments-Sorval, Miami, Florida) using a diamond knife. We chose

NIH-PA Author Manuscript

NIH-PA Author Manuscript

NIH-PA Author Manuscript

the width of the section, paralleling the Haversian canal direction, as the reference direction for the orientation of collagen. The specimens were placed on TEM grids.

Each TEM grid containing the specimens was placed on a STEM holder and examined using a Zeiss SUPRA VP-40 field emission scanning electron microscope (FESEM) equipped with a STEM detector at an accelerating voltage of 20 kV and at a working distance of 4 mm. The STEM rasters the focused incident probe across the specimen, which has been thinned to facilitate detection of electrons scattered through the specimen. The STEM detector enables pure bright field or extinct field imaging to achieve optimum contrasts and rich imaging details of unstained thin sections. Further, the transmission mode of the FESEM has the advantages of avoiding chromatic aberration, allowing for a larger aperture to obtain higher transmission, signal to noise ratio, and contrast enhancement due to the lower electron energy within the 10 to 30kV range. We observed and imaged the bone tissue at magnifications ranging between 6,000 and 54,000. We imported the images in XaraX software. We superimposed segments along the collagen bundles, and measured the magnitude of the smaller angle that the segment formed with the longitudinal reference line. The magnitude of the angle therefore varied between 0° and 90°.

Statistical analysis

We used statistical software package Stata (StataCorp LP, College Station, Texas) with the assistance of UCLA's Academic Technical Services Statistical Consulting Group. We expressed the data as mean ± standard error for all the measured parameters. The robustness of the morphometric method was analyzed through consideration of intra- and inter-observer errors relative to Haversian system area, whole osteon area, lamellar thickness, collagen length and collagen orientation, which involved manual marking to enable software detection for automatic measuring. To assess the magnitude of the intra-observer error, each parameter was measured on two specimens by one observer enough times (fifteen) to afford sufficient data to consider their distribution. The distributions did not show outliers or marked skewness. Therefore, the t-test was applied to compute the power of the mean to detect the actual measurements. Because we measured with a precision of 0.5%, the probability of the mean to provide the actual measurement ranged between 0.73 and 0.80. The error of not reflecting the actual measurement equals at most (max-min)/min, which was found between 0.005 and 0.007. The intra-observer error for a unique measurement was found to be less than 1%.

In the analysis of the inter-observer error between two independent observers measuring two specimens, the mean of the differences of corresponding measurements provided a power that ranged between 0.72 and 0.77 for the actual prediction of each measurement. The error of not reflecting the actual measurement equals at most (max-min)/min, between 0.006 and 0.008. The inter-observer error for a unique measurement on two specimens was found at most to be equal to 1%. On the basis of the 1% threshold of the above-analyzed morphometric errors, measurement by a single observer was considered appropriate.

After checking the normality of distributions, we used paired t-tests to establish significant differences between pre- and post- PTH(1-34) treatment for each of the input variables: average bright birefringence by CPL; percentage of whole osteons with specific birefringent

NIH-PA Author Manuscript

NIH-PA Author Manuscript

NIH-PA Author Manuscript

pattern (bright, semi-homogeneous, alternate extinct); average thickness of each of bright and extinct lamellae; and percent areas at specific degree of calcification (initial, intermediate-low, intermediate-high, and final) before and after PTH(1-34) treatment. We computed, in degrees, the collagen angle with respect to the longitudinal direction from the SCM data with the basic trigonometric formula:[53]

$$collagen\ angle = sin^{-1}(collagen\ length\ by\ SCM)/maximum(collagen\ lengths\ by\ SCM)$$

and compared these values with the experimental measurements of the same collagen angle obtained by STEM (Fig. 2). The correlation between collagen angles computed from collagen length data and experimentally obtained collagen angles was evaluated by the coefficient r^2. Because the two parameters of length of collagen bundles and collagen orientation within bright and extinct regions did not show a Gaussian distribution, we used the Kolmogorov-Smirnov test[54] to assess equality of distributions and non-parametric Chi-square statistics. For all the analyses, the level of significance was set at 0.05 before the Bonferroni adjustment for multiple comparisons.

Results

Collagen orientation underlying CPL birefringence by SCM and STEM

The bright and extinct birefringent signals of CPL were investigated by SCM and STEM, which allow the observation of the underlying distribution of collagen orientations. The length of the collagen bundles measured on SCM images (Fig. 2A–3C) within bright birefringent regions was statistically unchanged after PTH(1-34) treatment (0.28±0.01μm, 0.28±0.01μm; p=0.94). The length of the collagen bundles measured on SCM images within extinct birefringent regions was statistically unchanged after PTH(1-34) treatment (0.08±0.01μm vs. 0.07±0.01μm; p=0.38). The length of the collagen bundles differed between bright and extinct regions both before (bright, 0.22±0.02μm vs. extinct, 0.14±0.02μm, p=0.002), and after (bright, 0.21±0.02μm vs. extinct, 0.13±0.02μm, p=0.01), treatment, but there was no change due to the PTH(1-34) treatment itself.

We measured collagen orientation on STEM images of longitudinal sections prepared from regions that appear either birefringent bright or birefringent extinct in transverse section. The angle that collagen formed with the longitudinal direction on STEM images of longitudinal sections, within bright transverse regions (Figs. 2D-2G), clustered at 45°, with the majority (75±12% before and 73±9% after PTH(1-34) treatment, p=0.87) of the collagen bundles forming angles between 35° and 55°. The angle that the collagen bundles formed with the longitudinal direction within extinct transverse regions clustered at 10°, with the majority (82±10% before and 80±12% after PTH(1-34) treatment; p=0.39) of the collagen bundles forming angles between 0° and 23°. In particular, collagen orientation distribution differed significantly between bright and extinct birefringent regions both before (p=0.03), and after (p=0.04), PTH(1-34) treatment (Figs. 2F and 2G).

The collagen angles computed from the collagen length measured on SCM images correlated with the collagen angles measured on STEM images at bright regions (Figs. 2B,

NIH-PA Author Manuscript

NIH-PA Author Manuscript

NIH-PA Author Manuscript

2F, 2D) before (r^2= 0.73), and after (r^2=0.89), treatment with PTH(1-34) and at extinct regions (Figs. 2C, 2G, 2D) before (r^2= 0.94), and after (r^2= 0.98), treatment with PTH(1-34). Further, for bright regions, the computed collagen angles clustered at 45°, with the majority of the bundles forming angles between 35° and 55° (73±8% from SCM vs. 75±12% from STEM, p=0.63 before treatment; 83±7% from SCM vs. 73±9%, p=0.41 from STEM after treatment). For extinct regions, the computed collagen angles clustered at 10° with the majority (67±9% from SCM vs. 82±10% from STEM , p=0.22 before treatment; and 90±6% from SCM vs. 80±12% from STEM p=0.39, after treatment) of the collagen bundles forming angles between 0° and 23°.

RL and CPL microscopies

With PTH(1-34) treatment, the Harvesian system area changed from 11.92±5.82 to 12.76±4.50 (p=0.04) and the average brightness of CPL birefringence decreased from 0.45±0.02 to 0.40±0.01 (p=0.0005). Further, the number of whole osteons increased from 86.25±38.95 to 111.88 ±27.34 (p=0.02), and the osteon area was unchanged (62883.46±46064.64 vs. 45417.03±47477.82mm^2). After PTH(1-34) treatment, the average percentage of alternate osteons increased from 48.15±10.27 to 66.33±7.73 (p=0.034), in contrast with an insignificant decrease of semi-homogeneous (58.36±10.63 vs. 41±9.13, p=0.40) and bright (4.14±8.90 vs. 2.08±3.36, p=0.10) osteons (Table 2). With PTH(1-34) treatment, the thickness of osteons' bright lamellae increased from 3.78±0.11μm to 4.47±0.14μm (p=0.0002); and the thickness of osteons' extinct lamellae increased from 3.32±0.12μm to 3.70±0.12μm (p=0.045) (Fig. 3). The number of lamellae per osteon was unchanged (10.41±2.89 vs. 10.51±2.90).

CPL miscroscopy and micro-X-radiograph

The comparison of percentages of alternate osteons at same degree of calcification before and after treatment show an increase at each stage of calcification that brings the total percentage of alternate osteons to the 75 to 80% range: specifically, from 19.75±2.33% to 80.13±6.47% (p=0.0001) at initial stages of calcification, from 40.25±1.22% to 77.13±2.47% (p=0.0000001) at intermediate-low stage, from 30.25±3.47% to 74.75±2.67% (p=0.0000001) at intermediate-high stage, and from 50.38±1.28% to 74.88±5.43% (p=0.002) at final stage.

Discussion

We have evaluated cortical micro-structure, specifically the orientation of type I collagen and the degree of calcification, in biopsies from postmenopausal women with osteoporosis, before and after treatment with PTH(1-34). Our data confirm results on percent cortical porosity and degree of calcification obtained previously with different techniques.[25,55] Specifically, the percent cortical porosity measured here by high-resolution micro-Xray was similar to that previously measured by microCT.[25] Further, our data using micro-X-ray showed that the percent area of osteons at initial stages of calcification was increased by PTH(1-34) treatment, confirming a previous result by quantitative backscattered electron imaging.[55]

NIH-PA Author Manuscript

NIH-PA Author Manuscript

NIH-PA Author Manuscript

The techniques employed here for micro-structural investigation have been in development since the 1960s and have been applied mostly to basic science studies of human cortical bone.[42] The focus of the application in the current study has been the assessment of the variation of elementary components in iliac crest biopsies before and after treatment with PTH(1-34). In conformity with this line of investigation, the analysis was performed at increasing resolution to include variations within single osteons, and then within single lamella. We found a high degree of heterogeneity in Haversian system area, associated with a high degree of heterogeneity in number of osteons (r^2=0.92), compatible with the high degree of heterogeneity in the cortical thickness response among the same patients.[25] With PTH(1-34) treatment, the percentage increase in osteon ranges up to 116% with a mean±SE of 48.28±37.78. All patients had a similar response to treatment with respect to the other micro-structural parameters investigated: average brightness of CPL, osteon area, average percentage of alternate and non alternate osteons, lamellar thickness and distribution of degree of calcification.

We have analyzed the effect of PTH(1-34) on the orientation of collagen. At either bright or extinct birefringent regions, the lengths of collagen bundles obtained by SCM on the anterior-posterior/medial-lateral plane were reconciled with the assessment of the angles that collagen forms with the longitudinal direction by STEM (Fig. 2D). This allowed us to compute and check the collagen orientation on two planes perpendicular to each other. The observed collagen orientations differed between bright and extinct birefringent regions, similar to previous results at the femoral mid-shaft.[41] Previous results have demonstrated that both collagen orientation and the degree of calcification independently affect the mechanical properties of bone.[42,56–58]

The results of this study are compatible with the previously reported difference between bright and extinct birefringent lamellae at the femoral shaft in terms of orientations of collagen bundles that locally parallel the carbonated hydroxyapatite crystals. The observed orientations suggested the bright lamellae to be less resistant to axial tension and bending than the extinct lamellae.[56–58] This hypothesis was supported by the presence of collagen orientation patterns in the shaft of long bones where longitudinal collagen is dominant in regions that undergo tension. Collagen forming larger angles with the longitudinal direction is dominant in regions that undergo compression due to bending during walking.[45] The brightness and extinction of birefringence are indicative of the dominance of collagen orientation with respect to the longitudinal direction. On transverse section, a higher average brightness means a greater percentage of collagen fibrils forming large angles with the osteon axis, whereas a lower average brightness represents a greater extent of collagen bundles that form smaller angles with the osteon axis. After PTH(1-34) treatment, the average brightness decreased, representing an increase in collagen bundles forming small angles with the longitudinal direction.

Possible explanations of this change in orientation in relation to the complex mechanical stimulation at the iliac crest include an improvement of tissue response to loading or simply an expression of increased heterogeneity of orientations. In fact, with PTH(1-34) treatment, larger regions of alternating bright and extinct lamellae replace regions of brightness in semi-homogeneous and in bright osteons compared to pre-treatment samples. Such change

NIH-PA Author Manuscript

NIH-PA Author Manuscript

NIH-PA Author Manuscript

increases the variation of collagen orientation from location to location. Further, with PTH(1-34) treatment, the degree of calcification of osteons diversifies, with a higher number of osteons at initial degree of calcification relative to the rather homogeneous percentages of osteons at different degrees of calcification in the pre-PTH(1-34) treatment tissue. PTH(1-34) treatment brings the percentage of alternate osteons to the 75 to 80% range through percentage increases that are inversely proportional to the degree of calcification. PTH(1-34) treatment increases the proportion of osteons at initial stages of calcification, indicative of increased bone formation of osteons during remodeling, and reduce mean tissue age.

The lamellar thickness increase with PTH(1-34) treatment is a phenotype specific to the Haversian system. The lamellar thickness does not increase with PTH(1-34) treatment in either endocortical lamellae (3.58±0.64 vs. 3.71±0.72, p=0.14) or trabecular lamellae (3.45±0.76 vs.3.43±0.65; p=0.81). The increase in lamellar thickness observed with PTH(1-34) is unchanged by consideration of sub-grouping at specific stages of calcification (data not shown). Further, the lack of increase in lamellar number indicates that osteoblasts produce a standard number of lamellae. The lack of change in osteon surface area, compatible with the increase lamellar thickness and unchanged lamellar number because of the generally irregular osteon' s transverse section, leads us to hypothesize that the number of recruited osteoblasts that form an osteon is not affected by PTH(1-34) treatment. Because the number of osteons increases significantly with PTH(1-34) treatment and osteon size is unchanged, to increase cortical thickness, the balance of the increased number of osteons must form by remodeling of newly formed tissue. Therefore, the cortical tissue balance is modified by osteon number and, within the osteon, by lamellar thickness, and within endocortical bone, by lamellar number.

PTH(1-34) treatment has previously been found directly to stimulate bone formation without prior resorption on both endocortical and trabecular bone surfaces in postmenopausal women with osteoporosis.[59,60] Lindsay et al.[61] suggested that bone formation occurs either on previously quiescent surfaces or by osteoblast spillover, from remodeling sites, to previously quiescent surfaces. Further, with PTH(1-34) treatment, the lamellar number increases in both trabeculae and endosteal lamellar packets, which, in conjunction with the absence of change in lamellar thickness, is responsible for the significant increase of the width of lamellar packets of trabecular and endocortical bone, respectively.[22, 25] Since the area occupied by the Haversian system increases substantially with PTH(1-34) treatment, we conjecture that new woven bone may form first, with perhaps primary osteons at the endosteal surface, rich in osteoblasts, before remodeling in terms of secondary osteons takes place. The fact that we do not observe either woven bone nor primary osteons leads us to hypothesize that the three-year duration of the treatment afforded time for the woven bone to be remodeled with secondary osteon.

The rate of osteon formation during remodeling was previously hypothesized to be associated with the thickness of birefringent bright lamellae on transverse sections of alternating osteons.[62] The rate of osteon formation was previously found to decrease from cement line to Haversian canal [63]. The thickness of lamellae may depend on the level of activity of osteoblasts during the interval of time while lamellae are formed, which is the

NIH-PA Author Manuscript

NIH-PA Author Manuscript

NIH-PA Author Manuscript

time elapsing between the beginning of the osteoblasts' activity and the differentiation of osteoblasts into osteocytes. It is controversial whether lamellar thickness decreases from the cement line to the Haversian canal.[64,65] Nevertheless, if indeed osteons' lamellar thickness depends on formation rate, then PTH(1-34) treatment would increase formation rate of osteons' lamellae. The rate of osteon formation during remodeling has not been measured and will be matter of future studies.

Collagen concentration may be lower in lamellae that appear extinct in transverse sections, regardless of age and of PTH(1-34) treatment. Such difference in concentration is more apparent in lamellae isolated from the surrounding osteon and observed in the original radial direction of the osteon.[41] Although we have not quantified such concentrations, other investigators have shown by scanning electron microscopy a difference in collagen concentration in the two types of lamellae, and coined the terminology "collagen rich" for the lamella that appears extinct on transverse section, and "collagen poor" or "collagen loose" for the lamella that appears bright on transverse section.[66] Because we find a lower average bright birefringence after treatment with PTH(1-34), the bone tissue may be richer in collagen in comparison to pre-treatment. Collagen-richer tissue may increase flexibility and delay fractures.

These observed micro-structural changes are initial steps in understanding the reduced fracture risk observed with PTH(1-34) treatment.[5,9,10] Indeed, our data indicate that PTH(1-34) treatment correlates with distribution of birefringence, and therefore distribution of collagen orientation, in osteons through arrangement and thickness of extinct and bright lamellae.[41] In particular, PTH(1-34) treatment may result in an increasing presence of alternate osteons with thicker bright and extinct lamellae. The percentage of alternate osteons and thickness of both bright and extinct lamellae increase from pre- to post-treatment. An increased lamellar thickness in cortical bone may help to reduce fracture risk at weight bearing sites. Prior studies have shown a reduction in lamellar thickness in osteons at the femoral neck of patients with femoral neck fracture, in contrast to patients without femoral neck fracture.[39] An increase in lamellar thickness may increase the osteon stiffness by reducing the extent of the weaker lamellar interface.[67]

Other investigators have recently started to address heterogeneity of bone tissue in conjunction with the study of cortical tissue parameters at the site of atypical fractures in bisphosphonate-treated patients. In particular, Donnelly *et al*. have recently demonstrated the reduced compositional heterogeneity in bisphosphonate-treated bone.[68] It is also known that PTH treatment affects collagen cross-links.[69–71] It is possible that the reduced sensitivity of bone cells to detect mechanical stimulation in osteoporosis impedes the osteoblasts from producing a matrix with specific variations in terms of distributions of collagen orientation and degree of calcification, which would impair proper function and increase fracture risk.[72] The investigation of additional sub-micro-scale parameters that can affect fracture risk will be the subject of future studies.

This study is based on a small number of women, although the paired biopsy samples provide greater power than a cross sectional study. These women were all on long-term hormone/estrogen therapy when PTH(1-34) treatment was started. Whether this influenced

NIH-PA Author Manuscript

NIH-PA Author Manuscript

NIH-PA Author Manuscript

our findings in cortical bone is unclear. Studies of the effect of PTH on cortical bone of women who have not been on prior or continued antiresorptive therapy are being planned in order to investigate this point.

The mechanism of the anabolic effect of PTH is complex. Animal studies indicate that PTH(1-34) treatment induces a rapid increase in osteoblast number without proliferation of progenitor cells.[73] PTH treatment increases cortical bone mass, cross-sectional area, and endocortical surfaces in rat cortical bone.[11–14] Increased bone formation rate and mineralizing surface on the periosteal and endocortical surfaces have been found in rabbits.[15] Previous results on cortical bone show that the anabolic effect of PTH occurs primarily at the endocortical wall,[25] though periosteal apposition might also occur.[74] This study identifies elementary components of compact bone micro-structure as candidates to be checked for the reduction of fracture risk at weight bearing locations by PTH(1-34) treatment: both distribution of collagen orientation and degree of calcification are altered by PTH(1-34) treatment. These findings reinforce previous observations of collagen orientation and degree of calcification as optimally distributed in healthy bone tissue to withstand biomechanical demands, while pathological bone metabolism, such as that which occurs in postmenopausal women with osteoporosis, alters such distribution.[45,75–80]

Acknowledgments

Ascenzi designed the study, trained Lee and Liao, reviewed imaging and data analyses and wrote the paper. Lee, Liao and Billi conducted microscopy investigations and data collection. Dempster participated in the design of the study and analysis and interpretation of the histomorphometric data. Bilezikian, Cosman, Lindsay, Nieves and Zhou performed the clinical studies that provided the specimens. All the authors participated in the revision of the paper.

The authors thank John S. Adams for helpful discussions; Alessandro Corsi for preparation of micro-X-rays; Qian Zhang and Sinan Jabori for assistance with data analysis; Christian Seger and Matthew Schibler for assistance with SCM, performed at UCLA's CNSI Advanced Light Microscopy/Spectroscopy Shared Resource Facility, supported with funding from NIH-NCRR shared resources grant (CJX1-443835-WS-29646) and NSF Major Research Instrumentation grant (CHE-0722519). This work was partially supported by NIH grants NIDDK 32333 and NIDDK 069350 to John Bilezikian and AR39191 to Robert Lindsay.

References

1. Reeve J, Tregear GW, Parsons JA. Preliminary trial of low doses of human parathyroid 1–34 peptide in treatment of osteoporosis. Clin Endocrinol. 1976; 21:469–477.
2. Reeve J, Meunier PJ, Parsons JA, Bernat M, Bijvoet OLM, Courpron P, Edouard C, Lenerman L, Neer RM, Renier JC, Slovik D, Vismans FJFE, Potts JT. Anabolic effect of human parathyroid hormone fragment on trabecular bone in involutional osteoporosis: A multicentre trial. BMJ. 1980; 280:1340–1344. [PubMed: 6992932]
3. Slovik DM, Rosenthal DI, Doppelt SH, Potts JTJ, Daly MA, Campbell JA, Neer RM. Restoration of spinal bone in osteoporotic men by treatment with human parathyroid hormone (1–84) and 1,25 dihydroxyvitamin. J Bone Miner Res. 1986; 1:377–381. [PubMed: 3503551]
4. Finkelstein J, JS, Klibanski A, Schaefer EH, Hornstein MD, Schiff I, Neer RM. Parathyroid hormone for the prevention of bone loss induced by estrogen deficiency. N Engl J Med. 1994; 331:1618–1623. [PubMed: 7969342]
5. Lindsay R, Nieves J, Formica C, Henneman E, Woelfert L, Shen V, Dempster D, Cosman F. Randomized controlled study of effect of parathyroid hormone on vertebral-bone mass and fracture incidence among postmenopausal women on estrogen with osteoporosis. Lancet. 1997; 350:550–555. [PubMed: 9284777]
6. Hodsman AB, Fraher LJ, Watson PH, Ostbye T, Stitt LW, Adachi JD, Taves DH, Drost D. A randomized controlled trial to compare the efficacy of cyclical parathyroid hormone versus cyclical

NIH-PA Author Manuscript

NIH-PA Author Manuscript

NIH-PA Author Manuscript

parathyroid hormone and sequential calcitonin to improve bone mass in postmenopausal women with osteoporosis. J Clin Endocrinol Metab. 1997; 82:620–628. [PubMed: 9024265]

7. Roe EB, Sanchez SD, del Puerto A, Bachetti P, Cann CE, Arnaud CD. Parathyroid hormone 1–34 (hPTH 1-34) and estrogen produce dramatic bone density increases in postmenopausal osteoporosis - results from a placebo-controlled randomized trial. J Bone Miner Res. 1997; 14:S137.
8. Lane NE, Sanchez S, Modin GW, Genant HK, Ini E, Arnaud CD. Parathyroid hormone can reverse corticosteroid induced osteoporosis. Results of a randomized controlled clinical trial. J Clin Invest. 1998; 102:1627–1633. [PubMed: 9788977]
9. Cosman F, Nieves J, Formica C, Woelfert L, Shen V, Lindsay R. Parathyroid hormone in combination with estrogen dramatically reduces vertebral fracture risk. Osteopor Int. 2000; 11:S176.
10. Neer RM, Arnaud CD, Zanchetta JR, Prince R, Gaich G, Reginster J-Y, Hodsman AB, Eriksen EF, Ish-Shalom, Genant HK, Wang O, Mitlak BH. Effect of parathyroid hormone (1-34) on fractures and bone mineral density in postmenopausal women with osteoporosis. N Engl J Med. 2001; 344:1434–1441. [PubMed: 11346808]
11. Liu C-C, Kalu DN. Human parathyroid hormone (1–34) prevents bone loss and augments bone formation in sexually mature ovariectomized rats. J Bone Miner Res. 1990; 4:449–458.
12. Oxlund H, Ejersted C, Andreassen TT, Torring O, Nilsson MH. Parathyroid hormone (1–34) and (1–84) stimulate cortical bone formation both from periosteum and endosteum. Calcif Tissue Int. 1993; 53:394–399. [PubMed: 8293353]
13. Wronski TJ, Yen CF. Anabolic effects of parathyroid hormone on cortical bone in ovariectomized rats. Bone. 1994; 15:51–58. [PubMed: 8024852]
14. Baumann BD, Wronski TJ. Response of cortical bone to antiresorptive agents and parathyroid hormone in aged ovariectomized rats. Bone. 1995; 16:247–253. [PubMed: 7756054]
15. Hirano T, Burr DB, Turner CH, Sato M, Cain RL, Hock JM. Anabolic effects of human biosynthetic parathyroid hormone fragment (1–34), LY333334, on remodeling and mechanical properties of cortical bone in rabbits. J Bone Miner Res. 1999; 14:536–545. [PubMed: 10234574]
16. Andreassen TT, Ejersted C, Oxlund H. Intermittent parathyroid hormone (1–34) treatment increases callus formation and mechanical strength of healing rat fractures. J Bone Miner Res. 1999; 14:960–968. [PubMed: 10352105]
17. Andreassan TT, Willick GE, Morely P, Whitfield JF. Treatment with parathyroid hormone hPTH(1-34)(1-34), hPTH(1-34) (1-31) and monocyclic hPTH(1-34)(1-31) enhances fracture strength and callus amount, after withdrawal fracture strength and callus mechanical quality continue to increase. Calc Tiss Int. 2004; 74:351–356.
18. Kakar S, Einhorn TA, Vora S, Miara LJ, Hon G, Wigner NA, Toben D, Jacobsen KA, Al-Sebaei MO, Song M, Trackman PC, Morgan EF, Gerstenfeld LC, Barnes GL. Enhanced chondrogenesis and Wnt signalling in PTH(1-34)-treated fractures. J Bone Miner Res. 2007; 22:1903–1912. [PubMed: 17680724]
19. Tagil M, McDonald MM, Morse A, Peacock L, Mikulec K, Amanat N, Godfrey C, Little DG. Intermittent PTH(1-34) (1–34) does not increase union rates in open rat femoral fractures and exhibits attenuated anabolic effects compared to closed fractures. Bone. 2010; 46:852–859. [PubMed: 19922821]
20. Nakajima A, Shimoji N, Shiomi K, Shimizu S, Moriya H, Einhorn TA, Yamazaki M. Mechanisms for the enhancement of fracture healing in rats treated with intermittent low-dose human parathyroid hormone (1–34). J Bone Miner Res. 2002; 17:2038–2047. [PubMed: 12412812]
21. O'Loughlin PF, Cunningham ME, Bukata SV, Tomin E, Poynton AR, Doty SB, Sama AA, Lane JM. Parathyroid hormone (1–34) augments spinal fusion, fusion mass volume, and fusion mass quality in a rabbit spinal fusion model. Spine. 2009; 34:121–130. [PubMed: 19112335]
22. Bradbeer JN, Arlot ME, Meunier PJ, Reeve J. Treatment of osteoporosis with parathyroid peptide (h-PTH 1-34) and oestrogen: Increase in volumetric density of iliac cancellous bone may depend on reduced trabecular spacing as well as increased thickness of packets of newly formed bone. Clin Endocr. 1992; 37:282–289. [PubMed: 1424211]
23. Hodsman AB, Kisiel M, Adachi JD, Fraher LJ, Watson PH. Histomorphometric evidence of increased bone turnover without change in cortical thickness or porosity after 2 years of cyclical

NIH-PA Author Manuscript

NIH-PA Author Manuscript

NIH-PA Author Manuscript

hPTH(1–34) therapy in women with severe osteoporosis. Bone. 2000; 27:311–318. [PubMed: 10913928]

24. Jiang Y, Zhao JJ, Mitlak BH, Wang O, Genant HK, Eriksen EF. Recombinant human parathyroid hormone (1–34) [teriparatide] improves both cortical and cancellous bone structure. J Bone Miner Res. 2003; 18:1932–1941. [PubMed: 14606504]
25. Dempster DW, Cosman F, Kurland ES, Zhou H, Nieves J, Woelfert L, Shane E, Plavetić K, Müller R, Bilezikian J, Lindsay R. Effects of daily treatment with parathyroid hormone on bone microarchitecture and turnover in patients with osteoporosis: a paired biopsy study. J Bone Miner Res. 2001; 16:1846–1853. [PubMed: 11585349]
26. Ohishi M, Schipani E. PTH and stem cells. J Endocrinol Inv. 2011; 34:552–556.
27. Rashid G, Bernheim J, Green J, Benchetrit S. Parathyroid hormone stimulates the endothelial expression of vascular endothelial growth factor. Europ J Clinical Invest. 2008; 38:798–803. [PubMed: 19021696]
28. Sims NA. Building bone with a SOST-PTH partnership. J Bone Min Res. 2010; 25:175–177.
29. Guo J, Liu M, Yang D, Bouxsein ML, Saito H, Galvin RJ, Kuhstoss SA, Thomas C, Schipani E, Baron R, Bringhurst FR, Kronenberg HM. Suppression of Wnt signaling by Dkk1 attenuates PTH-mediated stromal cell response and new bone formation. Cell Metab. 2010; 11:161–171. [PubMed: 20142103]
30. Paszty C, Turner CH, Robinson MK. Sclerostin: a gem from the genome leads to bone-building antibodies. J Bone Min Res. 2010; 25:1897–1904.
31. Krause C, Korchynskyi O, de Rooij K, Weidauer SE, de Gorter DJ, van Bezooijen RL, Hatsell S, Economides AN, Mueller TD, Löwik CW, Dijke PT. Distinct modes of inhibition by sclerostin on bone morphogenetic protein and Wnt signaling pathways. J Biol Chem. 2010; 285:41614–41626. [PubMed: 20952383]
32. Hartmann C. A Wnt canon orchestrating osteoblastogenesis. Trends Cell Biol. 2006; 16:151–158. [PubMed: 16466918]
33. Pinson KI, Brennan J, Monkley S, Avery BJ, Skarnes WC. An LDL receptor-related protein mediates Wnt signalling in mice. Nature. 2000; 407:535–538. [PubMed: 11029008]
34. Wang EA, Rosen V, D'Alessandro JS, Bauduy M, Cordes P, Harada T, Israel DI, Hewick RM, Kerns KV, Lapan P, Luxenberg DP, Mcquaid D, Moutsatsos IK, Nove J, Wozney JM. Recombinant human bone morphogenetic protein induces bone formation. Proc Nat Acad Sci. 1990; 87:2220–2224. [PubMed: 2315314]
35. Bonnick, SL. Skeletal anatomy in densitometry. In: Bonnick, SL., editor. Bone Densitometry in Clinical Practice. New York, NY: Humana Press; 1998. p. 35-78.
36. Rockoff SD, Sweet E, Bleustein J. The relative contribution of trabecular and cortical bone to the strength of human lumbar vertebrae. Calcif Tissue Res. 1969; 3:163–175. [PubMed: 5769902]
37. Boutroy S, Van Rietbergen B, Sornay-Rendu E, Munoz F, Bouxsein ML, Delmas P. Finite element analysis based on in vivo HR-pQCT images of the distal radius is associated with wrist fracture in postmenopausal women. J Bone Min Res. 2008; 23:392–399.
38. Bonucci, E. Biological Calcification Normal and Pathological Processes in the Early Stages. Springer; Heidelberg, Germany: 2007.
39. Power J, Loveridge N, Lyon A, Rushton N, Parker M, Reeve J. Bone remodeling at the endocortical surface of the human femoral neck: a mechanism for regional cortical thinning in cases of hip fracture. J Bone Miner Res. 2003; 18:1775–1780. [PubMed: 14584887]
40. Ascenzi M-G, Ascenzi A, Benvenuti A, Burghammer M, Panzavolta S, Bigi A. Structural differences between "extinct" and "bright" isolated human osteonic lamellae. J Struct Biol. 2003; 141:22–33. [PubMed: 12576017]
41. Ascenzi M-G, Lomovtsev A. Collagen orientation patterns in human secondary osteons, quantified in the radial direction by confocal microscopy. J Struct Biol. 2006; 153:14–30. [PubMed: 16399238]
42. Ascenzi, M-G.; Benvenuti, A.; Ascenzi, A. Single osteon micromechanical testing. In: An, Y.; Draughn, R., editors. Mechanical Testing of Bone. CRC Press; Boca Raton, Florida, USA: 2000. p. 271-290.

NIH-PA Author Manuscript

NIH-PA Author Manuscript

NIH-PA Author Manuscript

43. Galilei, G. Discorsi e dimostrazioni matematiche intorno à due nuoue scienze attenenti alla mecanica & i mouimenti locali. Elzevir; Leiden: 1638. p. 128-130.(available at http://galileo.imss.firenze.it)
44. Leeuwenhoek, AV. An extract of a letter from Mr. Anth. Van. Leeuwenhoek containing several observations on the texture of the bones of animals compared with that of wood, on the bark of trees, on the little scales found on the cuticula, etc. Vol. 202. Philosophical Transactions of the Royal Society; London: 1693. p. 838-843.
45. Ascenzi A. The micromechanics versus the macromechanics of cortical bone – a comprehensive presentation. J Biomech Eng. 1988; 110:357–363. [PubMed: 3060679]
46. Silverberg SJ, Shane E, De La Cruz L, Dempster DW, Feldman F, Seldin D, Jacobs TP, Siris ES, Cafferty M, Parisien MV, Lindsay R, Clemens TL, Bilezikian JP. Skeletal disease in primary hyperparathyroidism. J Bone Miner Res. 1989; 4:283–291. [PubMed: 2763869]
47. Atkinson, PJ.; Hallsworth, AS. The spatial structure of bone. In: Harrison, RJ.; Navaratnam, V., editors. Progress in Anatomy. Vol. 2. University Press; Cambridge, Massachussetts, US: 1982. p. 179-199.
48. Ascenzi A, Bonucci E, Bocciarelli SD. Quantitative analysis of calcium in bone with a microradiographic method. Nuovo Cimento Series X. 1960; 18:216–220.
49. Amprino R, Engström A. Studies on x-ray absorption and diffraction of bone tissue. Acta Anat. 1952; 15:1–22. [PubMed: 14932636]
50. Engström A, Engfeldt B. Lamellar structure of osteons demonstrated by microradiography. Cell Mol Life Sci. 1953; 9:19.
51. Ascenzi A, Bonucci E, Bocciarelli DS. An electron microscope study on primary periosteal bone. J Ultr Res. 1966; 18:605–618.
52. Ascenzi A, Benvenuti A. Orientation of collagen fibers at the boundary between two successive osteonic lamellae and its mechanical interpretation. J Biomech. 1986; 19:455–463. [PubMed: 3745221]
53. Aufmann, RN.; Barker, VC.; Nation, RD. College Trigonometry. Cengage Learning, 2007. Florence; Kentuky, USA: p. 134-146.
54. Lehmann, EL.; Romano, J. Testing Statistical Hypotheses. Springer-Verlag; New York, New York, USA: 2008. p. 20-26.
55. Misof BM, Roschger P, Cosman F, Kurland ES, Tesch W, Messmer P, Dempster DW, Nieves J, Shane E, Fratzl P, Klaushofer K, Bilezikian J, Lindsay R. Effects of intermittent parathyroid hormone administration on bone mineralization density in iliac crest biopsies from patients with osteoporosis: a paired study before and after treatment. J Clin End Met. 2003; 88:1150–1156.
56. Ascenzi, A.; Bonucci, E.; Checcucci, A. The tensile properties of single osteons studied using a microwave extensimeter. In: Evans, FG., editor. Studies on the Anatomy and Function of Bone and Joints. Springer-Verlag; New York, New York, USA: 1966. p. 121-141.
57. Ascenzi A, Ascenzi M-G, Benvenuti A, Mango F. Pinching in longitudinal and alternate osteons during cyclic loading. J Biomech. 1997; 30:689–695. [PubMed: 9239548]
58. Ascenzi A, Bonucci E. The compressive properties of single osteons. Anat Rec. 1968; 161:377–392. [PubMed: 4879362]
59. Dempster DW, Zhou H, Cosman F, Nieves J, Adachi JD, Fraher LJ, Watson PH, Lindsay R, Hodsman AB. PTH treatment directly stimulates bone formation in cancellous and cortical bone in humans. J Bone Miner Res. 2001; 16(S1):S179.
60. Ma YL, Zeng Q, Donley DW, Ste Marie L, Gallagher JC, Dalsky GP, Marcus R, Eriksen EF. Teriparatide increases bone formation in modeling and remodeling osteons and enhances IGF-II immunoreactivity in postmenopausal women with osteoporosis. J Bone Min Res. 2006; 21:855–864.
61. Lindsay R, Cosman F, Zhou H, Bostrom MP, Shen VW, Cruz JD, Nieves JW, Dempster DW. A novel tetracycline labeling scheduling for longitudinal evaluation of the short-term effects of anabolic therapy with a single iliac crest bone biopsy: Early actions of teriparatide. J Bone Miner Res. 2006; 21:366–373. [PubMed: 16491283]
62. Ardizzoni A. Osteocyte lacunar size–lamellar thickness relationships in human secondary osteons. Bone. 2001; 28:215–219. [PubMed: 11182381]

NIH-PA Author Manuscript

NIH-PA Author Manuscript

NIH-PA Author Manuscript

63. Vincent J, Ngvete M. Les remaniements de l'os compact marqué à l'aide de plomb. Rev Belg Pathol. 1957; 26:161–170.
64. Marotti G. A new theory of bone lamellation. Calcif Tissue Int. 1993; 53:S47–S56. [PubMed: 8275380]
65. Ascenzi M-G, Andreuzzi M, Kabo JM. Mathematical modeling of secondary osteons. Scanning. 2004; 26:25–35. [PubMed: 15000289]
66. Marotti G, Muglia MA, Palumbo C. Structure and function of lamellar bone. Clin Rheumatol. 1994; 1:63–68. [PubMed: 7750244]
67. Simkin A, Robin G. Fracture formation in differing collagen fiber pattern of compact bone. J Biomech. 1974; 7:183–188. [PubMed: 4837554]
68. Donnelly, E.; Meredith, DS.; Gladnick, BP.; Rebolledo, BJ.; Lane, JM.; Boskey, AL. Reduced bone tissue heterogeneity with bisphosphonate treatment in postmenopausal women with fractures. 2010; Poster, 56th Annual Meeting of ORS;
69. Paschalis EP, Glass EV, Donley DW, Eriksen EF. Bone mineral and collagen quality in iliac crest biopsies of patients given teriparatide: new results from the fracture prevention trial. J Clin Endocrinol Metab. 2005; 90:4644–9. [PubMed: 15914535]
70. Paschalis EP, Shane E, Lyritis G, Skarantavos G, Mendelsohn R, Boskey AL. Bone fragility and collagen cross-links. J Bone Miner Res. 2004; 19:2000–2004. [PubMed: 15537443]
71. Saito M, Marumo K. Collagen cross-links as a determinant of bone quality: a possible explanation for bone fragility in aging, osteoporosis, and diabetes mellitus. Osteop Int. 2010; 21:195–214.
72. Mulvihill BM, Prendergast PJ. Mechanobiological regulation of the remodelling cycle in trabecular bone and possible biomechanical pathways for osteoporosis. Clin Biomech. 2010; 25:491–498.
73. Dobnig H, Turner RT. Evidence that intermittent treatment with parathyroid hormone increases bone formation in adult rats by activation of bone lining cells. Endocr. 1995; 136:3632–3638.
74. Lindsay R, Zhou H, Cosman F, Nieves J, Dempster DW, Hodsman AB. Effects of a one-month treatment with PTH(1-34) on bone formation on cancellous, endocortical, and periosteal surfaces of the human ilium. J Bone Min Res. 2007; 22:495–502.
75. Goldman HM, Bromage TG, Thomas CDL, Clement JG. Relationships among microstructural properties of bone at the human midshaft femur. J Anat. 2005; 206:127–139. [PubMed: 15730478]
76. Beraudi A, Stea S, Bordini B, Baleani M, Viceconti M. Osteon classification in human fibular shaft by circularly polarized light. Cells Tissues Organs. 2010; 191:260–8. [PubMed: 19776542]
77. Beraudi A, Stea S, Montesi M, Baleani M, Viceconti M. Collagen orientation in human femur, tibia and fibula shaft by circularly polarized light. Bone. 2009; 44:S320.
78. Cristofolini L, Taddei F, Baleani M, Baruffaldi F, Stea S, Viceconti M. Multiscale investigation of the functional properties of the human femur. Philos Transact A Math Phys Eng Sci. 2008; 366:3319–3341.
79. Riggs CM, Vaughan LC, Evans GP, Lanyon LE, Boyde A. Mechanical implications of collagen fibre orientation in cortical bone of the equine radius. Anat Embryol. 1993; 187:239–248. [PubMed: 8470824]
80. Ionova-Martin SS, Do SH, Barth HD, Szadkowska M, Porter AE, Ager JW III, Ager JW Jr, Alliston T, Vaisse C, Ritchie RO. Reduced size-independent mechanical properties of cortical bone in high-fat diet-induced obesity. Bone. 2010; 46:217–225. [PubMed: 19853069]

NIH-PA Author Manuscript
NIH-PA Author Manuscript
NIH-PA Author Manuscript

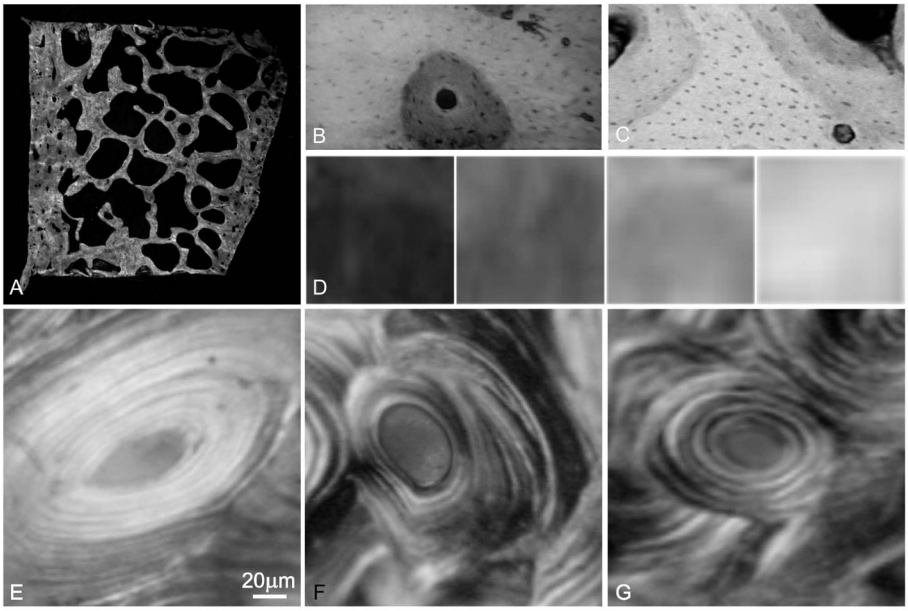

Figure 1.

(A) We assessed degree of calcification in transverse section of the iliac crest by high-resolution micro-X-ray. (B, C) Example of micro-structures at differing degrees of calcification classified as (D) initial, intermediate-low, intermediate-high, and final. Examples of organization of birefringent bright and extinct signals by CPL are shown in so-called (E) bright, (F) semi-homogeneous and (G) alternate osteons on transverse section. This example of (F) a semi-homogeneous osteon shows extinct regions that encompass portions of multiple lamellae, in contrast with an example of (G) an alternate osteon.

NIH-PA Author Manuscript

NIH-PA Author Manuscript

NIH-PA Author Manuscript

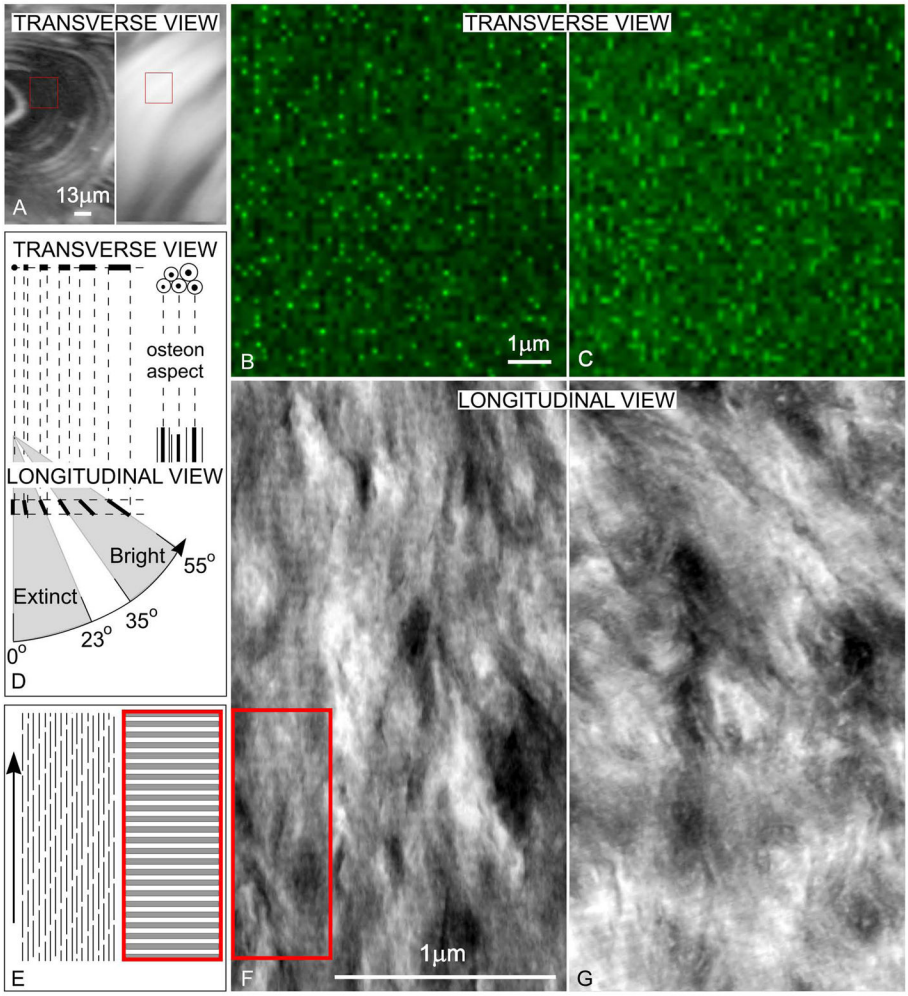

Figure 2.

(A) Regions (red rectangles) of extinct and bright birefringence by CPL in transverse sections are investigated by SCM: (B) corresponding to extinct, and (C) corresponding to bright, birefringence. Dots and short auto-fluorescent collagen are more numerous in extinct regions, while longer bundles are more numerous in bright regions. (D) The diagram explains relation of appearances of collagen bundles for each of extinct and bright regions between imaging by SCM (B, C) on transverse sections (where osteon aspect is circular or elliptical) and imaging by STEM (E, F) on longitudinal sections, cut along the general orientation of the Haversian canals, which defines the longitudinal direction. (E) STEM image corresponding to extinct birefringent transverse region shows longitudinal collagen pattern. (F) STEM image corresponding to bright birefringent transverse region shows collagen forming larger angles with the longitudinal direction.

NIH-PA Author Manuscript

NIH-PA Author Manuscript

NIH-PA Author Manuscript

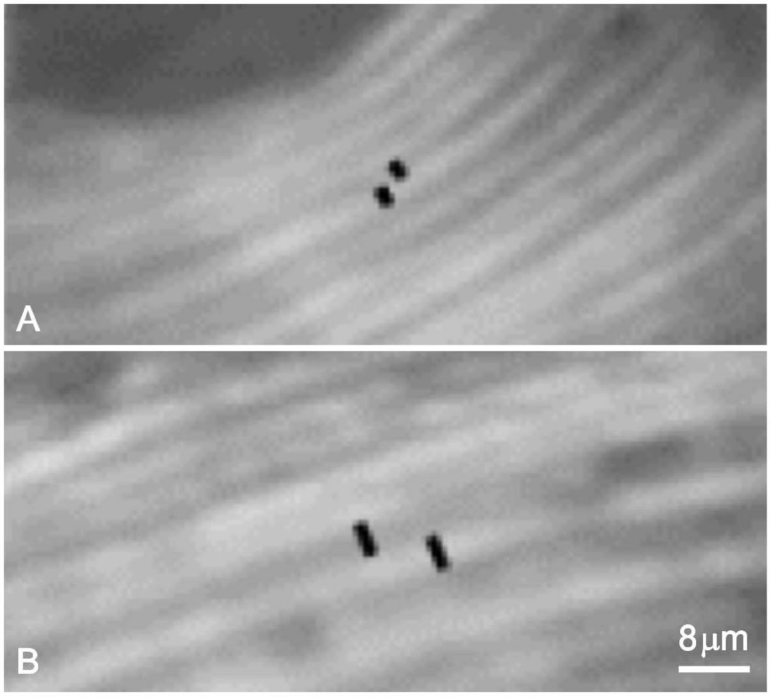

Figure 3.
Black segments are indicative of lamellar thickness of a bright, and of an extinct, lamella. (A) pre- and (B) post- PTH treatment.

NIH-PA Author Manuscript

NIH-PA Author Manuscript

NIH-PA Author Manuscript

Table 1

Age, cortical thickness and cortical porosity.

Group	Postmenopausal (n=8)		p-value (paired t-test)
	Pre-PTH	Post-PTH	
Age *(years)*	54.38±3.40	58.63±3.20	-
Cortical thickness *(μm)*	420±104	771±113	0.06
Cortical porosity *(% area)*	7.21±1.40	6.39±0.90	0.59

Values are reported as mean ± standard error. Cortical thickness and porosity were assessed by microCT in a previous study.[25]

NIH-PA Author Manuscript NIH-PA Author Manuscript NIH-PA Author Manuscript

Table 2

Measurements of bright and extinct birefringence and of micro-X-ray for cortices, osteons and lamellae.

Measurement	Type	Postmenopausal (n=8)		p-value (paired t-test)	
		Pre- PTH	Post- PTH		
Cortical birefringence *(from 0 to 1)*	Brightness	0.45±0.02	0.40±0.01	0.0005	
Osteon percent area *(%)*	Alternate	48.15±10.27	66.33±7.73	0.034	
	Semi-homogeneous	8.36±10.63	5.41±9.13	0.40	
	Bright	4.14±8.90	2.08±3.36	0.10	
Lamellar thickness *(μm)*	Bright	3.78±0.11	4.47±0.14	0.0002	
	Extinct	3.32±0.12	3.70±0.12	0.0017	
Cortical degree of calcification *(% area)*	Initial stages	42.87±8.03	57.16±3.08	0.89	0.04
	Intermediate-low	40.75±1.97	32.90±3.69		
	Intermediate-high	15.41±4.90	10.29±2.28	0.84	
	Final stages	3.63±1.23	2.86±0.44	0.75	
Alternate osteons (%)	Initial stages	19.75±2.33	80.13±6.47	0.0001	
	Intermediate-low	40.25±1.22	77.13±2.47	0.0000001	
	Intermediate-high	30.25±3.47	74.75±2.67	0.0000001	
	Final stages	50.38±1.28	74.88±5.43	0.002	

Values are reported as mean ± standard error. The number of the whole osteons varied between 37 and 150. There were between 6 to 15 lamellae per alternate osteon, meaning between 108 and 1485 lamellae per section.